THERMAL ANALYSIS OF NON-NEWTONIAN FLUID FLOW OVER SUPERHYDROPHOBIC SURFACE

By:
GAN ZHENG HONG
(Matrix No.: 128937)

Supervisor:
Dr. Yu Kok Hwa

May 2019

This dissertation is submitted to
Universiti Sains Malaysia
As partial fulfilment of the requirement to graduate with honours degree
in
BACHELOR OF ENGINEERING (MECHANICAL ENGINEERING)

School of Mechanical Engineering
Engineering Campus
Universiti Sains Malaysia

Declaration

This work has not been previously been accepted in substance for any degree and is not being concurrently submitted for any candidature for any degree.

Signed……. (Gan Zheng Hong)

Date…….

STATEMENT 1

This thesis is the result of my own investigations, except where otherwise stated.

Other sources are acknowledged by giving explicit references.

Bibliography/references are appended.

Signed……. (Gan Zheng Hong)

Date…….

STATEMENT 2

I hereby give consent for my journal, if accepted, to be available for photocopying and for interlibrary loan, and for the title and summary to be made available outside organizations.

Signed……. (Gan Zheng Hong)

Date…….

ACKNOWLEDGEMENT

Firstly, I am grateful and I would like to express my sincere gratitude to my supervisor, Dr Yu Kok Hwa for his guidance, encouragement and support throughout the research. My supervisor has provided me a clear direction and suggestion to achieve my objective and aims. His patient and encouragement has help and motivate me a lot in overcome the challenges faced during my research.

Secondly, I would like to show my appreciation School of Mechanical Engineering of University Sains Malaysia for provided me opportunities to improved and enhanced my practical skills and knowledges by conduct Final Year Project.

Last but not least, I would like to thank to my coursemate and family who have supported me in mental and physical throughtout the completion of this project.

TABLE OF CONTENTS

LIST OF TABLES

LIST OF FIGURES

Page

LIST OF SYMBOLS

C_p	Specific heat
D	Symmetric rate of shear tensor
D_H	Hydraulic diameter
E	Length of a period of alternating rib and groove
e	Length of the groove
F_b	Body Force
f	Fanning friction factor
H	Height for the inlet of plane channel
K	Consistency Index
k	Thermal Conductivity
L	Normalized groove-rib periodic spacing
L_h	Hydrodynamic Entrance Length
Lplaw	Development Length proposed by Fernandes et al. [26]
L_T	Thermal Entrance Length
n	Power-law index
p	Pressure
Re	Reynolds Number
Re_{gen}	Generalized Reynolds Number
U_{avg}	Average inlet velocity
u	Centerline velocity
U_B	Average inlet velocity
μ_{wall}	Viscosity of the wall
ρ	Density of Fluid
$\Phi(n)$	Simple hyperbolic function of the flow behavior index
ζ	Product of friction factor and the Reynolds Number

δ	Dimensionless gas area fraction
τ	Newtonian extra shear tensor
η	Dynamic viscosity
$\dot{\gamma}$	Function of second invariant of the rate of deformation tensor
ϕ	Energy of the viscous dissipation
$\vec{\nabla}.$	Vector of differential operator
$\vec{q}$	Vector of heat flux per unit area
$\frac{D}{Dt}$	Material derivative

ABSTRAK

Teknologi yang semakin canggih telah meningkatkan permintaan terhadap salutan hidrofobik dan komponen kecil. Kajian terbaru mendedahkan kesan superhidrofobik kepada bendalir bukan Newtonan bagi saluran bentuk bulat. Oleh yang demikian, kajian yang lebih lanjut diperlukan untuk memahami kesan superhidrofobik kepada bendalir bukan Newtonan bagi saluran bentuk lain. (Contoh: saluran rata). Kajian ini menunjukkan kesan salutan superhidrofobik kepada cecair non-newtonian bagi saluran bentuk rata melalui simulasi. Simulasi untuk panjang hidrodinamik dijalankan pada pelbagai Reynolds number $0.001<Re<100$, $0.5<n<1.5$ dan $0.125< \delta <0.875$ manakala simulasi untuk panjang hidrodinamik thermal dijalankan pada pelbagai Reynolds number $0.001<Re<0.007$, $0.6<n<1.3$ dan $0.125< \delta <0.875$.

Keputusan menunjukkan panjang hidrodinamik bagi aliran cecair non-newtonian dalam saluran bentuk rata yang mempunyai salutan hidrofobik meningkat semasa n dalam linkungan $0.5<n<0.9$ dan menurun bagi linkungan $1.0<n<1.5$. Selain itu, korelasi positif berlaku antara panjang hidrodinamik dengan Reynolds number dan delta, δ .

Di samping itu, korelasi positif juga dijumpai pada panjang hidrodinamik thermal dengan Reynolds number, delta (δ), dan n untuk aliran bendalir bukan Newtonan melalui saluran bentuk rata yang mempunyai salutan hidrofobik.

ABSTRACT

The advancement of technology has led to the demand for hydrophobic surface coating and miniature components. However, recent studies only reveal the effects of superhydrophobic surface on Non-Newtonian fluid for circular channel. Hence, there is a need for further the understanding of another type of channel (i.e, plane channel). This study presents a numerical investigation on the hydrodynamic entrance length and thermal entrance length of power-law fluid for planar channel flow consists of alternating superhydrophobic grooves and ribs arranged parallel to the flow direction. The simulations were performed in low Reynolds number range $0.001<Re<100$, for power-law index in the range of $0.5<n<1.5$ with dimensionless gas area fraction in the range of $0.125< \delta<0.875$ for hydrodynamic entrance length. On the other hands, the simulations for thermal entrance length were carried out in low Reynolds number range $0.001<Re<0.007$, for power-law index in the range of $0.6<n<1.3$ with dimensionless gas area fraction of $0.125< \delta<0.875$.

Numerical results show that the hydrodynamic entrance length for flow over superhydrophobic transverse grooves was longer compared to smooth wall for $0.5<n<0.9$ and shorter for $1.0<n<1.5$. Apart from that, it was found that the development length has a positive correlation with dimensionless gas area fraction and Reynolds numbers.

On the other hand, results show that the thermal entrance for planar channel flow having alternating ribs and grooves arranged parallel to the flow direction shows a positive correlation with Reynolds number, power-law index and dimensionless gas area fraction.

CHAPTER 1

INTRODUCTION

1.1 Overview

In this new era, science and technology have been rapidly developing. Application of microfluidic devices, wind tunnels, flow meters, and self-cleaning glass has received much attention. Such applications require the understanding of entrance length for the design and analysis flow. This is because the fluid and thermal performances such as velocity, temperature, Nusselt number, and velocity/dimensionless temperature profile in developing region would be continuosly changing, in contrast to that of fully developed region. Recent studies explored the effect of Newtonian fluid flow over superhydrophobic surface in the developing flow region. However, to the best of my knowledge, none of the studies reveals the effect of non-Newtonian fluid flow in plane channel consists of superhydrophobic surface in the developing flow region.

1.2 Superhydrophobic Surface

Nowadays, there are many practical applications including the use of water-repellent surface, including self-cleaning glass, anti-corrosion coatings, antifogging mirrors and etc [1]. Basically, superhydrophobic surface is a surface with a contact angle greater than 150°. This wetting condition occurs naturally. For instance, the water droplet on the lotus leaf will fall down from the surface of the leaf without wetting it [2]. The effect of superhydrophobic surface can be implemented by imposed an effective velocity slip length [3] or applied multiple boundary conditions [4]. Adoption of superhydrophobic coatings can reduce friction drag on the flow of the liquids. As a result, the overall of the mass flow rate is larger as compared to that of smooth surface [5]. Furthermore, it also influence the thermal entrance length and hydrodynamic entrance length. Generally, hydrodynamic entrance length is defined as the length from the inlet to the point where the inlet velocity reached 99% of its fully developed value [6] while thermal entrance length can be defined as the length before the fully thermal boundary layer developed [7].

1.3 Hydrodynamic entrance region and fully developed region

When a fluid flow between 2 parallel plates, the velocity of fluid particles in contact with the wall of the parallel plane are zero based on no-slip condition. These zero velocity fluids caused the velocity of nearby fluids decreased. However, the mass flow rate of the fluids is constant. Hence, the velocity of the centerline particles tends to increase. Therefore, the region when the velocity of the centerline fluids reached 99% of the fully developed velocity is called the hydrodynamic fully developed region and the region prior to its is terms hydrodynamic entrance region [7].

1.4 Thermal Entrance region and fully developed region

Consider fluids with uniform initial temperature flow between 2 parallel plates maintained at a temperature higher or lower than the inlet temperature. These unequal in temperature yields the development of thermal boundary layer. The thickness of the boundary layer will be increased until it reaches center of the plates. The region before the boundary layer reaches the center of the plates is known as thermal entrance region and the area after it is called thermal fully developed region [7].

1.5 Newtonian and Non-Newtonian Fluids

Fluids can be classified into 2 types, Newtonian or non-Newtonian. Newtonian fluid can be defined as the fluids with constant viscosity and the shear rate of Newtonian fluid is directly proportional to the shear stress [8]. On the other hand, non-Newtonian fluid is a fluid with a shear rate not directly proportional to the shear stress. Common example of Newtonian fluid and non-Newtonian fluid are emulsion and chocolates respectively [9].

1.6 Problem Statement

The usage of hydrophobic surface in applications (i.e., lab-on-chip technology, thermal management, self-cleaning, etc.) has been a subject of interest. In chemical and processing industries, many of the fluids use need to be heated or cooled. Since

many fluids used exhibit non-Newtonian behavior and the influence of these microstructures on developing flow is still largely unknown. Hence, this study will investigate the developing flows in planar channel flow have superhydrophobic transverse grooves and explore the thermal analysis of non-Newtonian fluids over the water-repellent surface.

1.7 Objectives

The few objectives are

1. To explore the effect of gas fraction on the hydrodynamic entrance length and thermal entrance length for non-Newtonian fluid in planar channel flow containing superhydrophobic transverse groove.
2. To explore the effect of Reynold number on the hydrodynamic entrance length and thermal entrance length for non-Newtonian fluid in planar channel flow containing superhydrophobic transverse groove.
3. To explore the effect of power law index (n) to the hydrodynamic entrance length and thermal entrance length for non-Newtonian fluid in planar channel flow containing superhydrophobic transverse groove.

1.8 Scope of the Project

In this project, the hydrodynamic entrance length and thermal entrance length of non-Newtonian fluid flow between planar channel with superhydrophobic grooves will be determined. Simulation will be carried out to determine velocity and temperature profile of the flows inside the channel by using Ansys 18.1. The range of power-law-index of the fluids is limited between 0.5 to 1.5 for hydrodynamic entrance length and 0.6 to 1.4 for thermal entrance length due to computational power of the central processing unit. The simulation results will be compared with correlation equation from previous studies for validation. MATLAB is used to simulate the data to obtain the hydrodynamic and thermal entrance length.

CHAPTER 2

LITERATURE REVIEW

2.1 Introduction

The development of the flow requires an axial distance from the inlet of tube or channel depends on inlet velocity profile or wall conditions. In addition to the understanding on fluid dynamics, the heat transfer of the fluids inside the pipe or channel is also important due to wide applications in industries. For instance, flow meters need a fully developed condition in order to work properly. Hence, by knowing the hydrodynamic entrance length, the required section for the developing of flow can be added before the flow meter [10]. Next, the measurement in a wind tunnel required a steady, uniform and fully developed flow. Thus, the understanding of hydrodynamic entrance length is important in design of the wind tunnels [11]. Moreover, microelectronic devices have rapid growth. The understanding of heat transfer is thus important. In this chapter, the previous studies by the researcher on hydrodynamic and thermal entrance length will be investigated.

2.2 Physical mechanism of the flow

Firstly, the fluids entering the channel or tube with a designated inlet velocity profile subjected to no-slip velocity condition at walls. As a result, the fluid particles in proximity to the wall slowed down due to viscous effects. Since the total mass flow rate of the fluids remains constant, the velocity of the fluid in the center increased to maintain conservation of mass. Eventually, the flow is fully developed once the flow is steady [12].

2.3 Summary of works from researcher for Newtonian flows

Numerous studies have been carried out by many researchers on the development length for laminar flows in pipe. The studies involved various methods, including analytical methods, numerical methods, and experimental methods. Table 2.1 shows a summary of the research conduct previously.

Table 2.1: Summary of research on development length of laminar pipe flow as presented by Durst et al. [12].

No.	Authors	Year	Method	L/D
1	Boussinesq [8]	1891	Analytical, two-zone approach	0.065 Re
2	Schiller [2]	1922	Integral approach, assuming a parabolic velocity distribution within the boundary layer	0.0288 Re
3	Atkinson and Goldstein [10]	1938	Analytical, generalization of the Blasius's solution of the flat plate	0.065 Re
4	Langhaar [3]	1942	Analytical, linearized the momentum equation	0.0575 Re
5	Nikuradse [9]	1950	Experiment	0.0625 Re
6	Siegel [11]	1953	Analytical, integral approach, assuming a cubic velocity distribution within the boundary layer	0.030 Re
7	Bogue [12]	1959	Analytical, integral approach, assuming a quartic velocity distribution within the boundary layer	0.0288 Re
8	Campbell and Slattery [14]	1963	Analytical, applying a plus viscous dissipation of energy term to the entire flow	0.0675 Re
9	Collins and Schowalter [15]	1963	Analytical, developing the work of Boussinesq	0.061 Re
10	Sparrow et al. [4]	1964	Analytical, utilizing a stretched axial coordinate and introducing a mechanical energy equation	0.056 Re
11	Hornbeck [16]	1964	Numerical, initial value problems	0.057 Re
12	McComas and Eckert [17]	1965	Experimental, by relating the pressure drop to distance from the pipe entry	(0.03–0.035)Re
13	Christiansen and Lemmon [18]	1965	Numerical, by obtaining a comparative numerical solution of the momentum equation	0.0555 Re
14	Vrentas et al. [19]	1966	Numerical, boundary value problem	0.056 Re
15	McComas [20]	1967	Analytical, general method depends only on knowledge of the fully developed velocity profile	0.026 Re
16	Friedmann et al. [21]	1968	Numerical, assuming that the initial velocity profiles are concave in the core rather than uniform	0.056 Re
17	Atkinson et al. [22]	1969	Numerical, finite element method	0.59+0.056 Re
18	Lew and Fung [6]	1970	Analytical, two sets of eigenfunctions	0.065 Re(Re < 1) 0.08 Re(Re > 50)
19	Fargie and Martin [23]	1971	Numerical, simplified the momentum equations by employing differential and integral form	(0.049–0.068)Re
20	Chen [24]	1973	Analytical, integral momentum method	(0.052–0.068)Re
21	Gupta [25]	1977	Numerical	0.0675 Re
22	Mohanty and Asthana [7]	1979	Analytical, two-zone approach to the inlet and filled regions	0.075 Re

From Table 2.1, it is clear that most of the entrance length was obtained analytically. The proposed correlation equation between normalized hydrodynamic entrance length and reynold number is $L/D=C$ Re. Figure 2.1 shows the results of constant C obtained by previous researches.

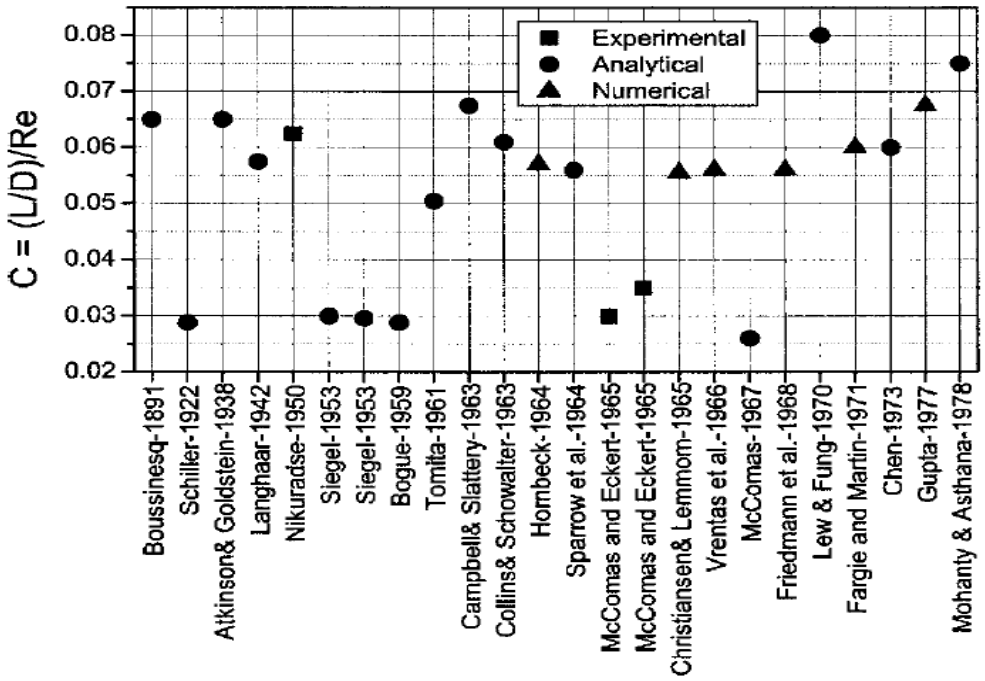

Figure 2.1: Results of constant C with various reynold number and normalized rntrance length [12]

However, literature of Atkinson et al. proposed a new correlation, which is $\frac{L}{D} = Co + C_1 Re$ [13] and this correlation is proved to be correct correlation equation since equation $L/D=C$ Re did not consider the effect of diffusion to the axial flow of the fluids, especially at lower Reynolds number. Ultimately, Durst et al. [12]. proceed the research in this area and eventually shows that the correlation equation between normalized entrance length and Reynolds number for pipe flow and channel flow which is valid throughout the practical range of Reynolds number.

Pipe Flow: $$\frac{L}{D} = [(0.631)^{1.6} + (0.0567Re^{1.6})]^{\frac{1}{1.6}} \quad (2.1)$$

Channel Flow: $$\frac{L}{D} = [(0.631)^{1.6} + (0.0442Re^{1.6})]^{\frac{1}{1.6}} \quad (2.2)$$

2.4 Summary of works from researcher for non-Newtonian flows

For power-law model, most of the researchers in early stage predict a relationship of normalized entrance length and Reynolds number as:

$$XD/D = C(\mathrm{Re})$$

where C=f(n) and n is the power-law index.

The problem of this correlation is that it neglects the effect of diffusion, especially when the Reynolds number is low. According to R.J. Poole [14], this correlation perhaps is only valid for Reynolds number with a value of 20 above. Besides that, these studies give an error of about ±10% [14]. Figure 2.2 shows the summary of research on development length for pipe flow of non-newtonian power law model.

Table 1 Summary of previous investigations of development-length requirements for non-Newtonian power-law pipe flows

Author	Method	Parameter range	Re definition	Re range	$X_D=f(\mathrm{Re})$	Newtonian prediction
Collins and Schowalter [3]	A	$0<n<1$	Re_{CS}	No range provided	$X_D/D=C(\mathrm{Re})$ where $C=f(n)$	$X_D/D=0.061(\mathrm{Re})$
Mashelkar [11]	A	$0<n<1$	Re_{CS}	"High Re"	$X_D/D=C(\mathrm{Re})$ where $C=f(n)$	$X_D/D=0.049(\mathrm{Re})$
Soto and Shah [12]	N	n=0.5, 0.75 and 1.5	Re_{CS}	No range provided	$X_D/D=(0.15-0.085n)\mathrm{Re}$[a]	$X_D/D=0.065(\mathrm{Re})$
Matros and Nowak [13]	A	No limit provided	Re_{MR}	No range provided	$X_D/D=\mathrm{Re}\left\{0.0865\left[\frac{2(n+1)}{3n+1}\right]^{-2}\right\}$	$X_D/D=0.0865(\mathrm{Re})$
Mehrota and Patience [14]	N	$0.6<n<1.5$	Re_{MR}	>200	$X_D/D=0.056(\mathrm{Re})$	
Ookawara et al. [15]	N	No limit provided	Consult ref	<50	$X_D/D=\sqrt{((0.655)^2+(0.0575)^2(\mathrm{Re})^2)}$	
Gupta [16]	A	$0.3<n<2.0$	Re_{MR}	No range provided	$X_D/D=C(\mathrm{Re})$ where $C=f(n)$	$X_D/D=0.04(\mathrm{Re})$
Chebbi [17]	A	$0<n<1.5$	Re_{CS}	No range provided	$X_D/D=C(\mathrm{Re})$ where $C=f(n)$	$X_D/D=0.09(\mathrm{Re})$

[a]Extracted by the current authors from graphical data

Figure 2.2: Summary of previous studies on development length for pipe flow of non-Newtonian fluid [14]

R.J. Poole further the studies of developing pipe flow for inelastic non-Newtonian fluids obeying the power-law model by numerical investigation. Ultimately, he proposed that the new correlation between hydrodynamic entrance length and Reynold number which is valid for power-law index in the range of 0.4<n<1.5 and Reynolds number in the range of 0<Re<1000.

2.5 Definition of Reynolds number

The first type of commonly used Reynolds number is Collins-Schowalter Reynolds number. This Reynolds number based on characteristic shear rate $\gamma=UB/D$, it came from simple dimensional analysis of the problem. However, it only valid in some cases and not always a preferred choice.

$$Re = \frac{\rho {U_B}^{2-n} D^n}{K}$$

The second type of Reynold number is the generalized Reynolds number, $\mathrm{Re}_{gen.}$ It is defined by Metzer and Reed and can be obtained by solving the momentum equation for simple ducts. (circular ducts or infinite parallel plate) [15].

$$Re_{gen} = \frac{\rho {U_B}^{2-n} {D_H}^n}{K\Phi(n)^n \zeta^{n-1}} \quad (2.3)$$

$$\frac{f}{2}Re_{gen} = \zeta \qquad (2.4)$$

For circular ducts,

$$\Phi(n) = \frac{3n+1}{4n} \qquad (2.5)$$

$$\zeta = 8$$

For infinite parallel plate,

$$\Phi(n) = \frac{2n+1}{3n} \qquad (2.6)$$

$$\zeta = 12$$

The third type of Reynolds number is suitable for turbulent flow. The advantage of this definition is that it based on the parameter within the flow but its disadvantage is that it needed comprehensive details of the flow.

$$Re = \frac{\rho U_B D}{\mu_{wall}}$$

2.6 Superhydrophobic Surface

There were 2 ways to imposed superhydrophobic surfaces effect. The first method is alternating micro-grooves and ribs arranged parallel to the flow direction. This is because when a surface is coated with hydrophobic material, the liquid was prevented from penetrate the cavities between micro-protrusions or nano-protrusions. As a result, vapor or air-pockets exists in the cavities. The presented of this vapor or air-pockets can reduce the contact area between the liquid and the wall and the results are reduction of flow resistance [16]. Figure 2.3 shows the superhydrophobic surfaces consist of alternating ribs and grooves arranged parallel to flow direction.

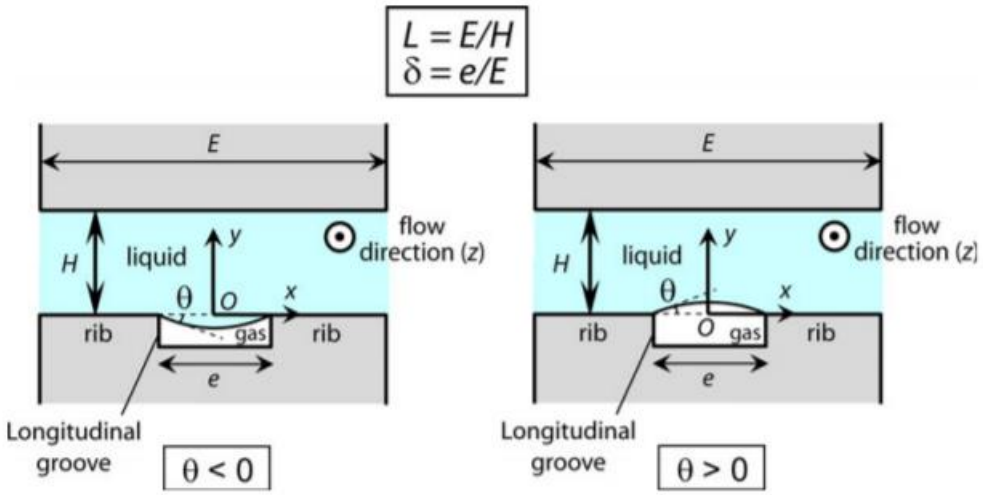

Figure 2.3: Superhydrophobic surface consist of alternating ribs and grooves arranged parallel to flow direction [16]

The second methods are implement arbitrary velocity slip length. This slip length can be understood as estimated length from the wall that the slip velocity profile enlarged outside the boundary as depicted in Figure 2.4 [17].

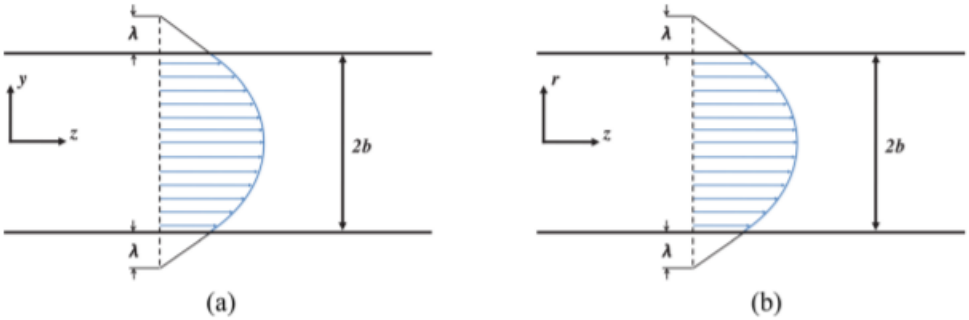

Figure 2.4: Velocity profile in a) simple channel b) tube [17]

2.7 Some research involved the superhydrophobic surface

There is few investigations involve the use of superhydrophobic surface. Firstly, Yu et al. [18] carried out an investigation about the influence of gas area fraction on developing flow in a pipe containing superhydrophobic transverse grooves. This study is carried by using numerical simulation to explore the effect of various gas fraction to the hydrodynamic entrance length. This study reveals the facts that increase in gas fraction can significantly reduce the flow friction resistance. Besides that, it also shows the effects of superhydrophobic grooves on the velocity profiles, velocity distribution along the centerline and hydrodynamic entrance length [18]. Moreover, another

investigation is also carried out by Yu et al.[19] on the development flow of power-law index in pipe consists of superhydrophobic transverse grooves. In the paper, the effect of development of velocity profile, centerline velocity distribution and hydrodynamic entrance length of power-law fluid due to the superhydrophobic transverse grooves are investigated [19]. Furthermore, a study on the flow inside plane channel flow with water-repellent surface containing transverse groove and ribs is also existed [20]. Similarly, the investigation shows the effect of present of water repellent surface to the velocity profile, centerline velocity distribution and hydrodynamic entrance length.

2.8 Summary of research involved the thermal analysis

The studies on the thermal entrance length have been done by many researchers. For instance, based on the article thermal entrance length and Nusselt number in coiled tube, the peripherally average Nusselt number is maximum at the inlet and decrease monotonically in the downstream direction. However, the peripherally average Nusselt number undergoes spatial oscillations before settling down to a fully developed value. They proposed the reasons for non-monotonic behavior of the peripherally average Nusselt number and show that at the region where the temperature field is everywhere uniform immediately following entry, the heat transfer is dominated by thermal diffusion from the wall [21]. Based on the research of thermal entrance length for non-Newtonian fluids in turbulent pipe flow, they reveal the fact that viscous non-Newtonian fluids require approximately the same thermal entrance length as Newtonian fluids. However, the entrance length for viscoelastic non-Newtonian fluid is seven times greater than Newtonian fluids [22]. An important study has been done by Owen T. Hanna. The study shows the equation to obtain the thermal entrance length for flow overs parallel plane, rectangular channel, and concentric annuli for constant surface heat flux [23]. Besides that, Poh.et al. [24] proposed a correlations use to predict local and average Nusselt numbers for laminar flow of Newtonian fluid through rectangular channel. The correlation shows a good agreement with available experiment data [24]. Moreover, the study of Poh et al. [24] shows that the local Nusselt number is decreased with the increase of axial distance and channel aspect ratio. However, the curve of nusselt number become increasingly flat when the aspect ratio and axial distance increase, as show in Figure 2.5 [24].

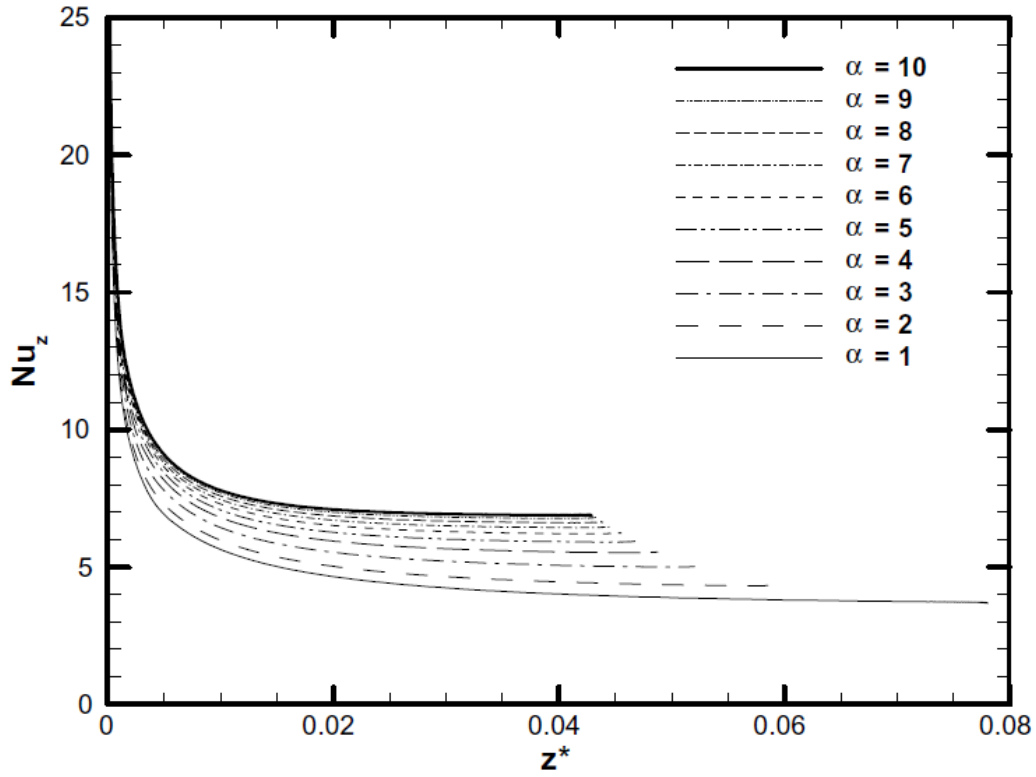

Figure 2.5: Local Nusselt Number as a function of dimensionless length and aspect ratio [24].

In addition, study of I.Vinogradov et al.[25] shows the observation of relative Nusselt number for heat transfer of non-Newtonian in rectangular channel. In this research, the change of relative Nusselt number is depends on the Prandtl number, power-law-index. When the Prandtl number is low ($Pr=10^2$), Nusselt number for shear thinning fluids is higher than nusselt number of Newtonian fluid but Nusselt number for shear thickening fluids is lower than Newtonian fluid. However, the trend is inverse where the Nusselt number of shear thinning fluids and shear thickening fluids is lower and higher than nusselt number of Newtonian fluids respectively when the Prantdl number is high ($Pr=10^4$). Similarly, the Nusselt number for the heat transfer in a plane channel is also found to be decreased along the channel and circular ducts, as observed in Hassen et al. [26] and Hayes et al.[27].

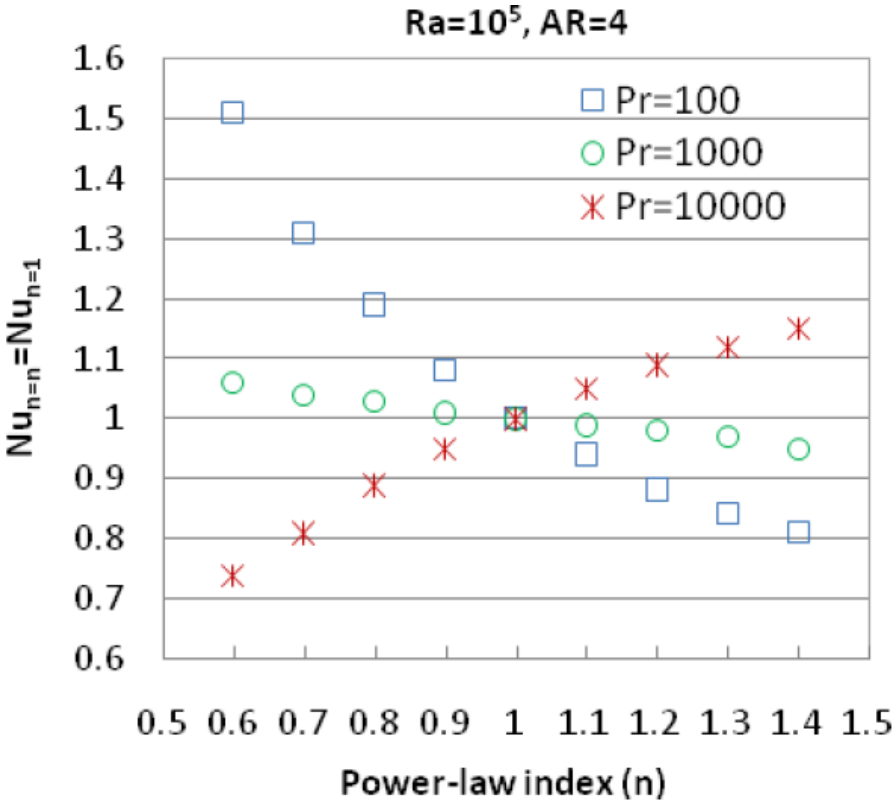

Figure 2.6: Plot of relative Nusselt number and power-law index(n) for various Prandtl number [25].

CHAPTER 3

METHODOLOGY

3.1 Introduction

There are 2 sections presented in this chapter. The first part is the determination of hydrodynamic entrance length and the second part is the determination of the thermal entrance length. Both sections utilized Ansys workbench to simulate the laminar flow in the planar channel for power-law fluid and Matlab R2018b to further process the simulation results.

3.2 Determination of hydrodynamic entrance length

3.2.1 Geometry of the model

Ansys Design Modeller is used to create the model. The model is a two-dimensional planar channel, as depicted in Figure 1. The height and length of the channel are 0.001m and 0.01m respectively. The wall of the channel consists of alternating groove and rib along the flow direction. To mimic the superhydrophobic surface, shear-free condition is applied to the groove and no-slip condition is applied to the wall. Besides that,velocity inlet and pressure outlet is applied for the entrance and exit of the fluids from the channel. There is a total of 100 periods of rib and grooves along the wall. The ratio between the length of rib and groove is termed dimensionless gas area fraction while the ratio between the length of a period of rib and groove is terms normalized groove-rib periodic spacing [20].

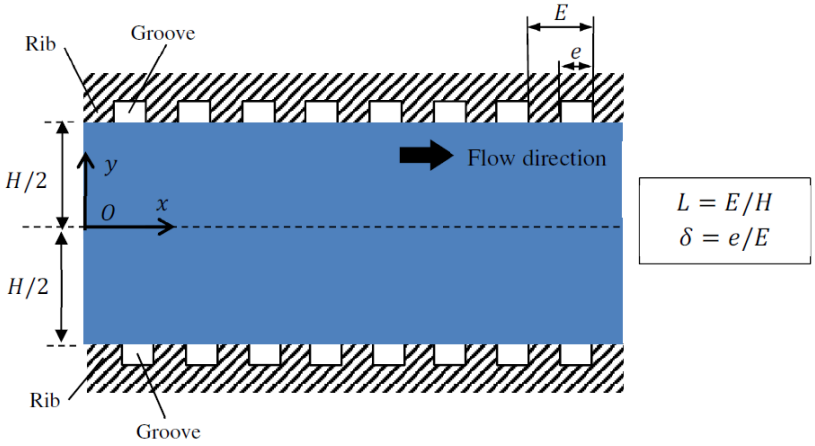

Figure 3.1: Geometry of the simulation model [20]

3.2.2 Grid-independent test

In this study, the variables, including power-law index, density, gas area fraction and Reynold number, is predefined. The number of the cells is determined by grid independent test. Four mesh size, 400 (x-direction)×20 (y direction), 800×40, 1600×80, and 3200x80 are employed to determine the hydrodynamic entrance length. The number of cells that give insignificant change in value of hydrodynamic entrance length when compared to other mesh size is employed in this study.

3.2.3 Properties of the fluid

The type of fluid in this study is not-Newtonian fluid with power-law-index between 0.5 to 1.5. The other properties of the fluid are shown in Table 3.1:

Table 3.1: Properties of the fluid

Density (kg/m^3)	1000
Consistency Index,k	1
Minimum Viscocity Limit (kg/ms)	0
Maximum Viscosity Limit (kg/ms)	1×10^{10}

3.2.4 Mathematical Model and governing equation

In this study, the flow of the fluid is assumed to be steady, laminar and incompressible. Hence, this flow can be governed by the continuity and momentum equation.

Continuity equation

$$\Delta.u= 0 \tag{3.1}$$

Momentum conservation

$$\rho\frac{\delta u}{\delta t} + \rho\nabla.(uu) = -\nabla p + \nabla.\tau \tag{3.2}$$

$$\tau= \eta\,(\nabla u + \nabla u^{T}) = 2\eta\mathbf{D} \tag{3.3}$$

$$\eta(\dot{\gamma})= \mu+K\dot{\gamma}^{n-1} \tag{3.4}$$

3.2.5 Solver Setting and solution method

Equation 3.1 to 3.4 is solved by Ansys Fluent 18.1, a finite volume based computational fluid dynamics (CFD) software package. Simple scheme is used to solve pressure and velocity coupling. The pressure and momentum solution is based on second order and second order upwind. The details of the solver setting and solution method are shown in Figure 3.3 and Table 3.2. The simulation is stopped once the residual of continuity, x-velocity and y-velocity reached as low as 1×10^{-08}.

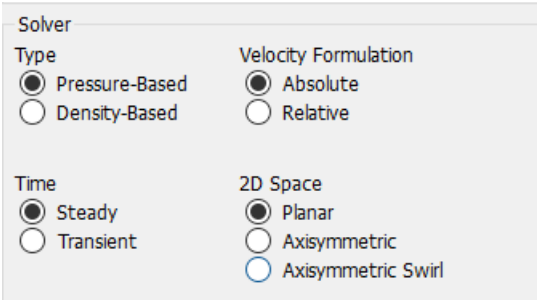

Figure 3.3: Setting of the solver

Tabe 3.2: Solution Methods

Solution Methods Pressure-Velocity Coupling	
Scheme	Simple
Spatial Discretization	
Gradient	Least Squares Cell Based
Pressure	Second Order
Momentum	Second Order Upwind

3.2.6 Reynolds Number

The generalized Reynold number was employed in this study. The Reynolds number is defined so that the Fanning factor, f = $\frac{12}{Re_{gen}}$ in laminar flow. It can be used to correlate the pressure fall needed to drive the fully developed flow of non-Newtonian fluid in plane channel [28].

$$Re_{gen} = \frac{6\,\rho U^{2-n}H^{n}}{K}\left(\frac{4n+2}{n}\right)^{-n} \tag{3.5}$$

3.2.7 Validation of Numerical Result

A graph of hydrodynamic entrance length versus Reynold numbers is plotted. The results is compare with correlation equation proposed by Fernandes et al [29]. Figure 3.4 shows an example of the validation plot and Equation (3.6) is the correlation equation use to validate the numerical result.

$$\text{Lplaw} = [\text{f(n)}^{1.6} + (0.0444 Re_{gen})\text{g(n)}]^{\frac{1}{1.6}} \quad (3.6)$$

$$\text{f(n)} = \frac{-0.355}{1+2e^{-(4..273n-0.553)}} - e^{-(15.706n-4.002)} + 0.981 \quad (3.7)$$

$$\text{g(n)} = -0.209n^2 + 0.645n + 1.225 \quad (3.8)$$

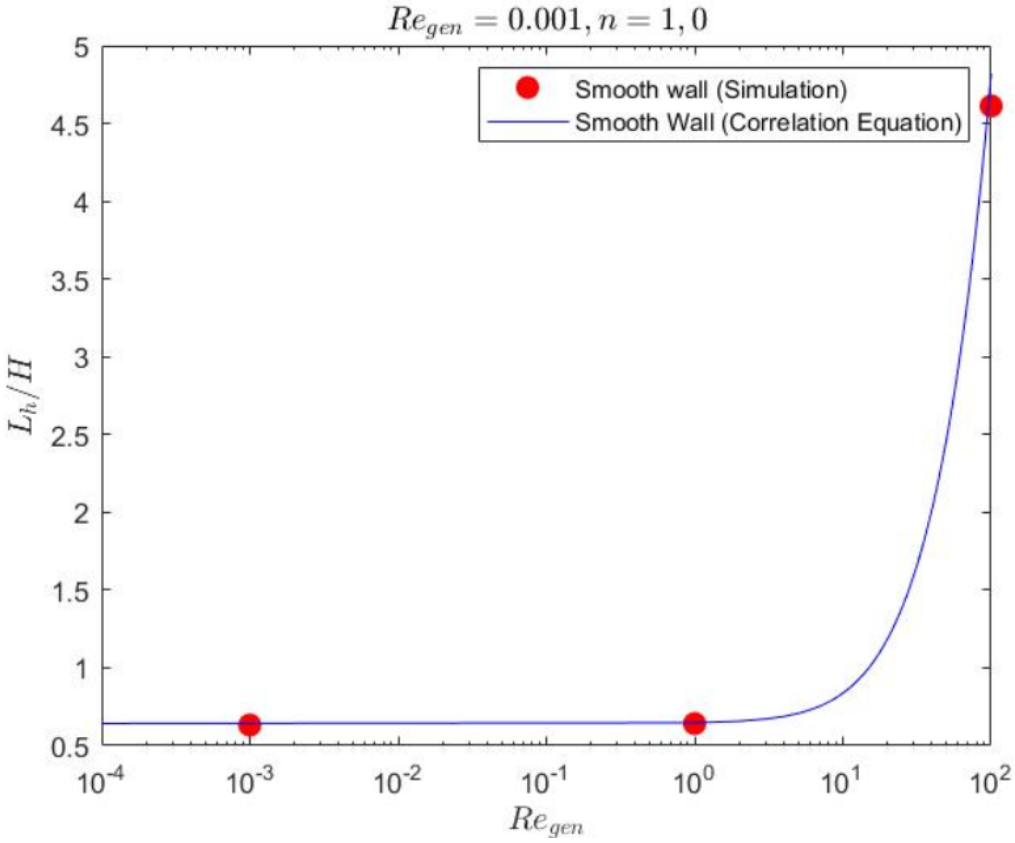

Figure 3.4: Validation Plot

3.2.8 Flow chart for the determination of hydrodynamic entrance length

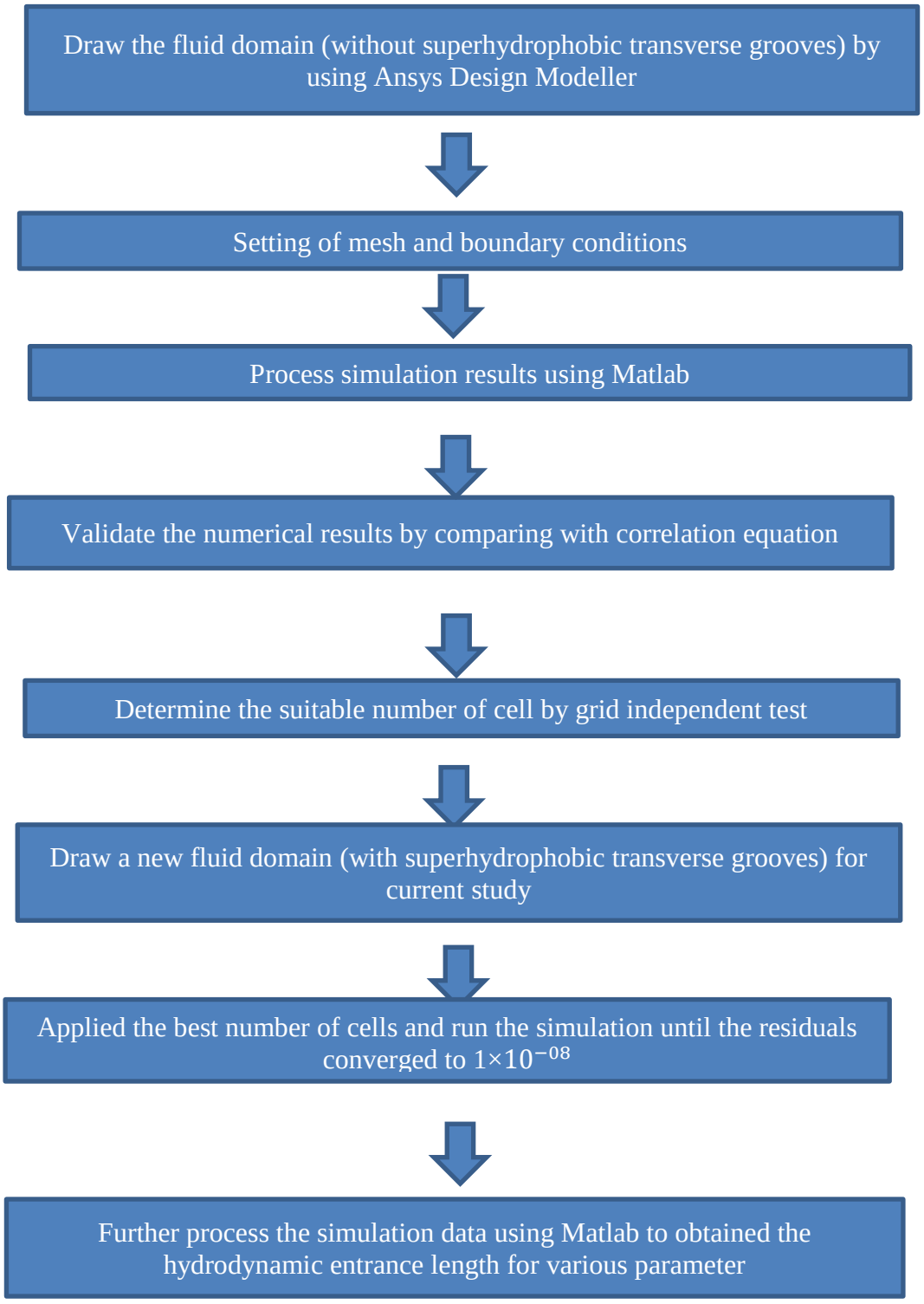

3.3 Determination of thermal entrance length

3.3.1 Geometry of fluid domain

The fluid domain consists of alternating ribs and grooves along the transverse direction. The height and the length if the channel is 0.001m and 0.02m, respectively. Constant wall temperature is applied along the solid-liquid interface but adiabatic condition is assumed along the liquid-gas interface. Similarly, shear-free condition is utilized to represent the exists of superhydrophobic surface. Besides that, velocity inlet and pressure outlet is applied for the entrance and exit of the fluids.

3.3.2 Properties of the fluids

The type of fluid in this study is not-Newtonian fluid with power-law-index between 0.6 to 1.4. The inlet temperature of the fluid is 300K. The other properties of the fluid are shown in Table 3.3:

Table 3.3: Properties of fluids

Density (kg/m^3)	1000
C_p, specific heat (J/kgK)	3900
Thermal Conductivity (W/mK)	0.595
Consistency Index,k	1
Minimum Viscocity Limit (kg/ms)	0
Maximum Viscocity Limit (kg/ms)	1×10^{10}

3.3.3 Mesh setting

The fluid domain was meshed using quadratic elements. A grid independent test is carried out to determine the suitable number of cells to be used in the entire simulation. Mesh sizes of 400 (x-direction) × 20 (y-direction), 800x40, 1600x80 and 3200x80 are use to determined the thermal entrance length. The grid sizes that gives lower variation in thermal entrance length will be selected as the suitable mesh sizes in this study.

3.3.4 Solution Method

The continuity and Navier-Stokes equation along with the boundary conditions were solved by Ansys Fluent 18.1, a finite volume based computational fluid dynamics (CFD) software package. 2 models were activated, which are energy and laminar models.

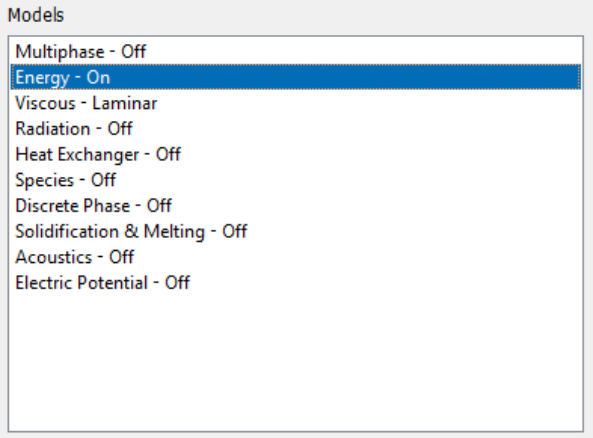

Figure 3.5: Models to be set

Simple scheme algorithm is used to solve pressure and velocity coupling. The momentum and energy equation was solved based on second-order upwind to ensure high accuracy. The simulation is run until the residuals (continuity, x-velocity and y-velocity, energy) converged to 1×10^{-08}. The details of the other setting are shown in Figure 3.6 and 3.7.

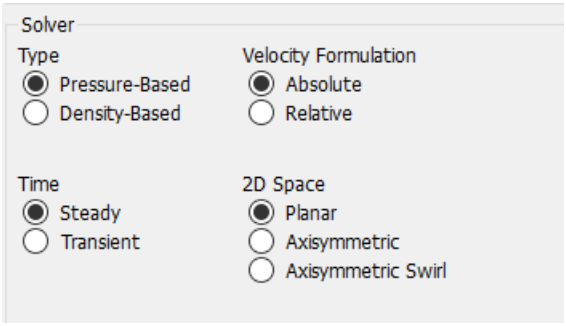

Figure 3.6: Solver setting

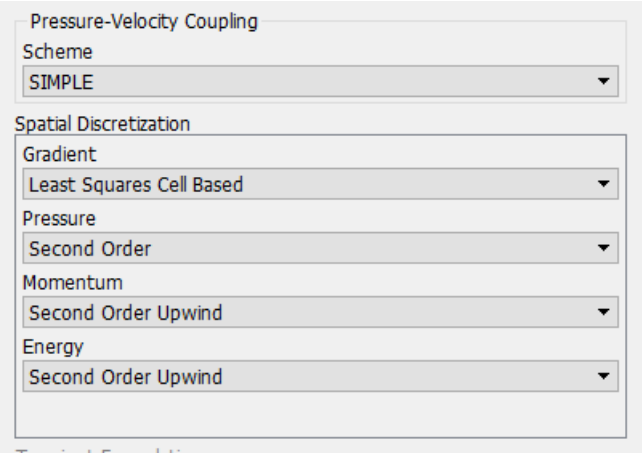

Figure 3.7: Solution Methods

3.3.5 Mathematical Model and governing equation

In this study, a few assumptions are made to model the heat transfer in the plane channel:

1	Steady State
2	Incompressible fluid
3	Laminar flow
4	Constant fluid properties
5	Negligible radiative and natural convective heat transfer

The heat transfer of the fluids can be governed by the continuity, momentum and energy equation.

Continuity Equation:

$$\frac{\delta \rho}{\delta t} = -\nabla . (\rho \overrightarrow{V}) \quad (3.9)$$

Conservation of Momentum:

$$\rho \frac{D\vec{V}}{Dt} = -\nabla p + \overrightarrow{F_b} + \overrightarrow{\nabla} . \tau \quad (3.10)$$

Energy Conservation Equation:

$$\rho \frac{DE}{Dt} = -\overrightarrow{\nabla} . \vec{q} - p\overrightarrow{\nabla} . \vec{V} + \phi \quad (3.11)$$

3.3.6 Flow chart for the determination of thermal entrance length

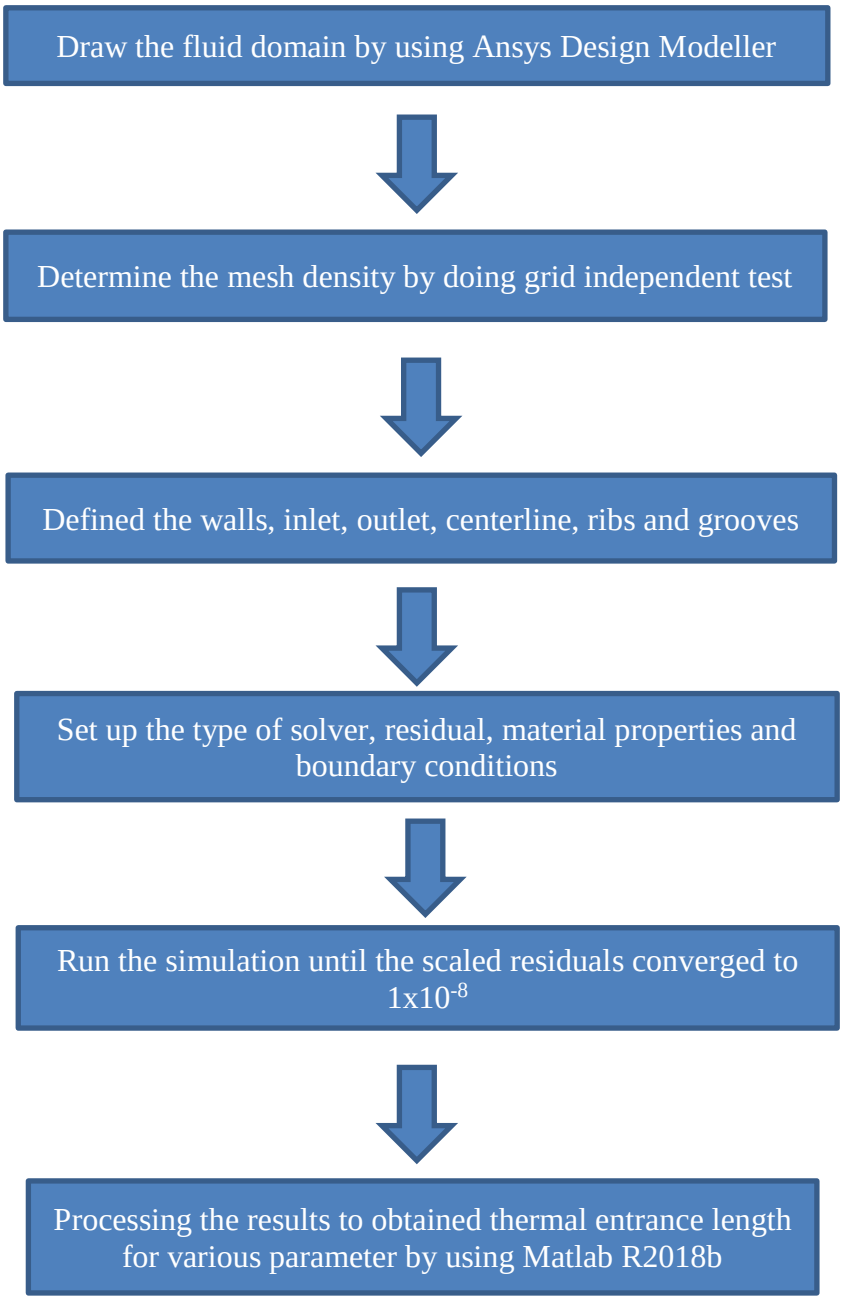

CHAPTER 4

RESULTS AND DISCUSSION

4.1 Validation of Numerical Results

Figure 4.1 shows the plot of variation of normalized hydrodynamic entrance length with Reynold numbers for flow of non-Newtonian fluid in-plane channel. The power-law-index of the fluid is 1. On the figure, the blue line shows the nonlinear correlation plot proposed by Fernandes et al [29]. From figure 4.1, it is obvious that a good agreement exists between the simulation and correlation. The largest and lowest percentage difference between the simulation data and correlation proposed by Fernandes et al [29] is about 4.31% and 0.87% respectively. This error is slightly higher than the average relative error of Fenandes et al [29], which is 3.7%. The details of the percentage difference for respective Reynold numbers is presented in Table 4.1.

Table 4.1: Percentage difference between normalized hydrodynamic entrance length and correlation for various Generalized Reynolds number

Generalized Reynolds numbers	Percentage difference between normalized hydrodynamic entrance length and correlation (%)
0.001	1.59
1	0.87
100	4.31

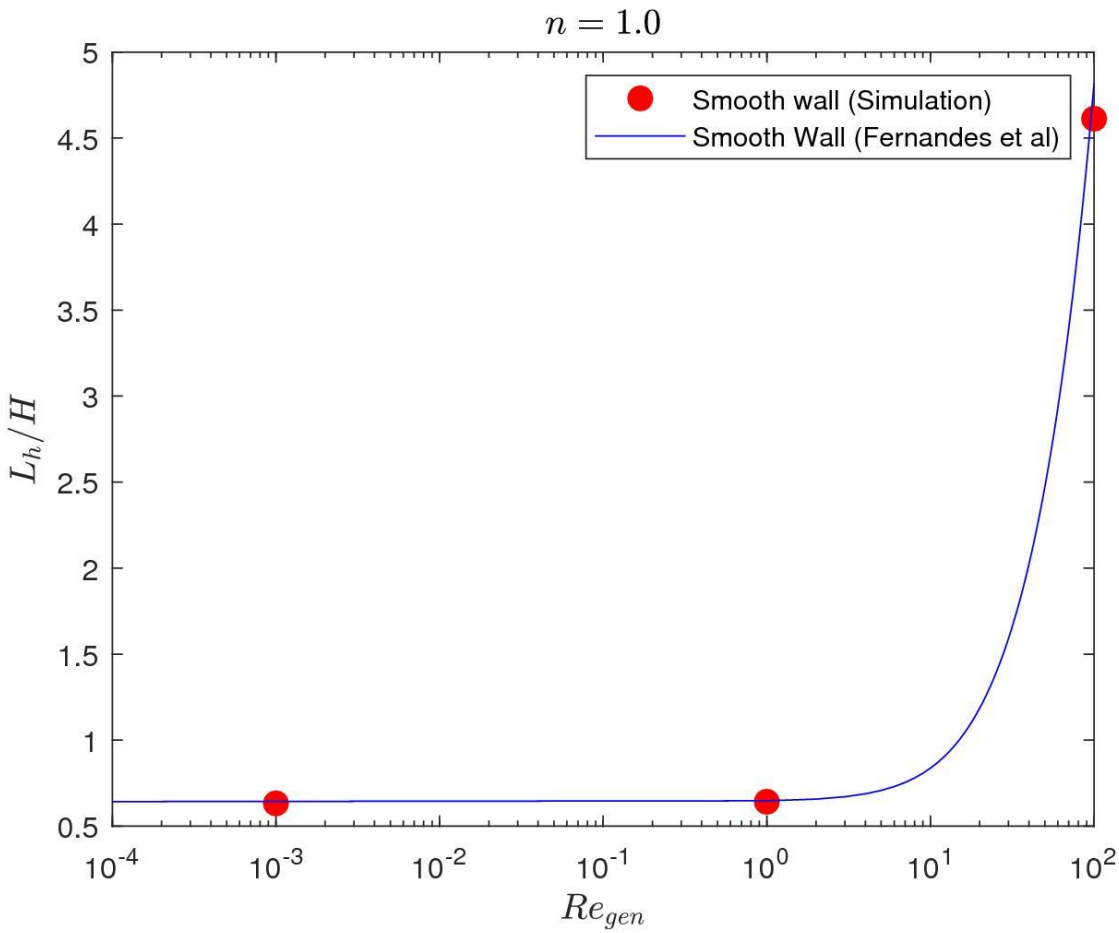

Figure 4.1: Plot of hydrodynamic entrance length for different generalized Reynolds number

4.2 Grid-independent test (hydrodynamic entrance length)

A grid independent test is performed to investigate the grid dependence and mesh density of the numerical solution for flow of power-law fluid in-plane channel having superhydrophobic grooves. The simulations are conducted for four grid resolutions, 400x20, 800x40, 1600x80 and 3200x160 quadrilateral cells. The first number represents the number of elements in the x-direction and the second number represents the number of elements in the y-direction. Furthermore, this simulation is performed for superhydrophobic transverse grooves with normalized groove-rib periodic spacing, L=0.1 and dimensionless gas area fraction, δ=0.5. The results are plotted in figure 13. From figure 4.2, it is clear that the solution converges as resolution increased. Increase the grid resolution from 1600x80 to 3200x160 yield a results with variation of 0.2980%. Hence, grid resolution of 1600x80 is employed in this study.

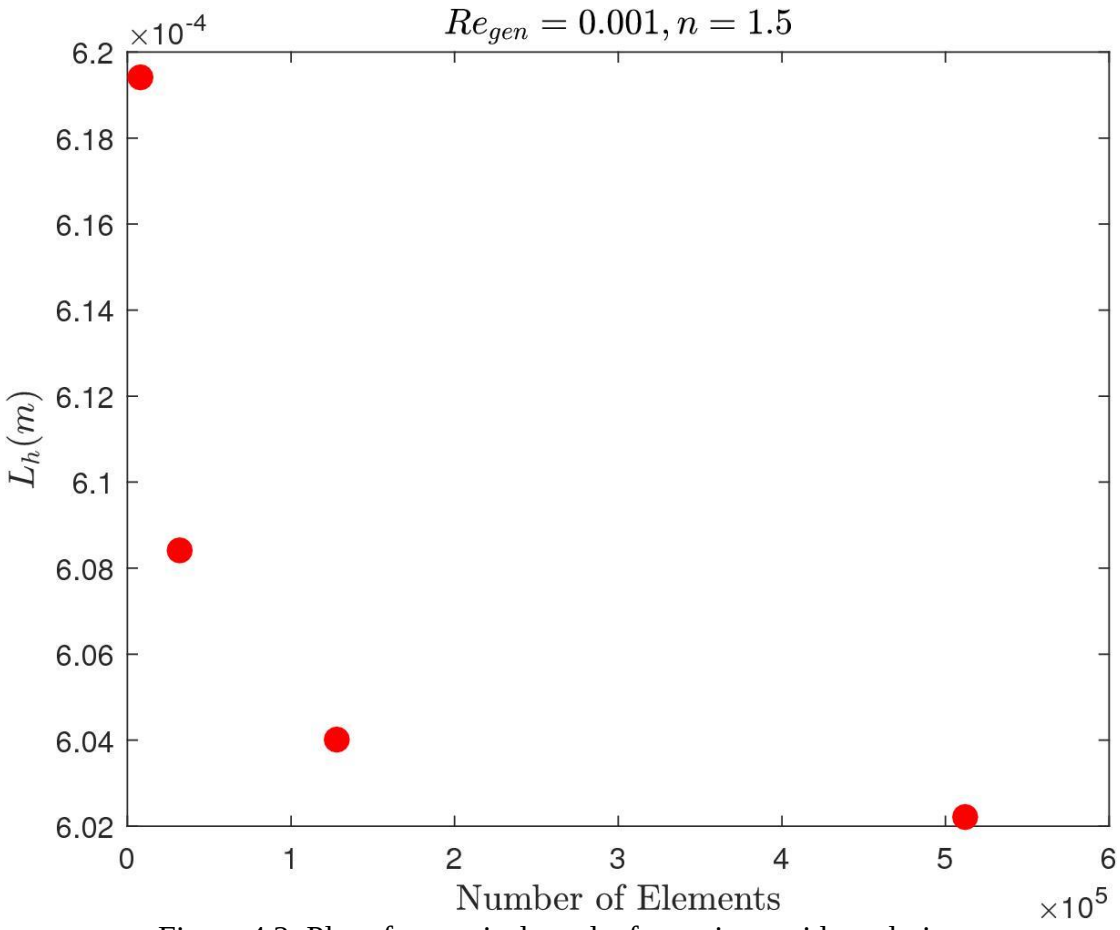

Figure 4.2: Plot of numerical results for various grid resolution

4.3 Effect of hydrodynamic entrance length

Figure 4.3 shows the plot of normalized hydrodynamic entrance length and power-law index. It can be seen that the normalized hydrodynamic entrance length decreases with the increase of power-law index. This is similar to the results obtained by Fernandes et al. [29], as shown on the blue line in Figure 4.3 where the normalized entrance length increases up to 0.5 and follows by a decrease. This phenomenon can be explained by Poole and Ridley [14]. When the Reynolds number is very low, the development length is dominated by diffusion. Hence, the increase in diffusion time when the power-law index decrease results in the increase of hydrodynamic entrance length [14]. Besides that, a more parabolic profile for fully developed velocity profile will happen when n increase. Consequently, more time or longer length is needed for the restrictive effect of the walls get to the center of the plane channel. However, the viscosity of the fluid increase as power-law index increased. The increase in viscosity